

ARPES spectral functions and Fermi surface for $\text{La}_{1.86}\text{Sr}_{0.14}\text{CuO}_4$ compared with LDA+DMFT+ $\Sigma_{\mathbf{k}}$ calculations

I.A. Nekrasov¹, E.E. Kokorina¹, E.Z. Kuchinskii¹, M.V. Sadovskii¹,
S. Kasai³, A. Sekiyama³, S. Suga³

¹*Institute for Electrophysics, Russian Academy of Sciences, Ekaterinburg, 620016, Russia*

³*Graduate School of Engineering Science, Osaka University, Toyonaka, Osaka 560-8531, Japan*

(Dated: October 4, 2018)

Slightly underdoped high- T_c system $\text{La}_{1.86}\text{Sr}_{0.14}\text{CuO}_4$ (LSCO) is studied by means of high energy high resolution angular resolved photoemission spectroscopy (ARPES) and combined computational scheme LDA+DMFT+ $\Sigma_{\mathbf{k}}$. Corresponding one band Hubbard model is solved via dynamical mean-field theory (DMFT), while model parameters needed are obtained from first principles within local density approximation (LDA). An “external” \mathbf{k} -dependent self-energy $\Sigma_{\mathbf{k}}$ describes interaction of correlated electrons with antiferromagnetic (AFM) pseudogap fluctuations. Experimental and theoretical data clearly show “destruction” of the LSCO Fermi surface in the vicinity of the $(\pi,0)$ point and formation of “Fermi arcs” in the nodal directions. ARPES energy distribution curves (EDC) as well as momentum distribution curves (MDC) demonstrate deviation of the quasiparticle band from the Fermi level around $(\pi,0)$ point. The same behavior of spectral functions follows from theoretical calculations suggesting AFM origin of the pseudogap state.

PACS numbers: 74.72.-h; 74.20.-z; 74.25.Jb; 31.15.A-

I. INTRODUCTION

One of the not yet solved puzzles of cuprate high-temperature superconductors (HTSC) is a nature of underdoped normal state - the pseudogap regime¹. Perhaps most powerful experimental tool to access electronic properties of the pseudogap state is angular resolved photoemission spectroscopy (ARPES)^{2,3,4}. Common understanding is the fluctuating origin of the pseudogap state, however type of the fluctuations is still under discussion. Whether these are superconducting fluctuations⁵ or some order parameter fluctuations (AFM(SDW), CDW, stripes, etc.)^{6,7} coexisting or competing with Cooper pairing is up to now undecided.

There are several prototype compounds among high- T_c systems e.g. hole doped $\text{Bi}_2\text{Sr}_2\text{CaCu}_2\text{O}_{8-\delta}$ (Bi2212) system or the electron doped one - $\text{Nd}_{2-x}\text{Ce}_x\text{CuO}_4$ (NCCO). Now a lot of experimental ARPES data on Bi2212 and NCCO is available (see the review Ref. 2). For instance Fermi surface (FS) maps, quasiparticle band dispersions and even self-energy lineshapes mapped onto some models are obtained from modern ARPES measurements⁶. Into this list of prototype compounds should be of course included the first ever high- T_c hole doped system $\text{La}_{2-x}\text{Sr}_x\text{CuO}_4$ (LSCO) which was also investigated both in theory and experiment with great details.²

Within the normal underdoped phase (pseudogap regime) a number of interesting physical phenomena were discovered. For example, FS is partially “destroyed” in the vicinity of the so-called “hot-spots” (points of crossing between FS and AFM unklapp surface). “Shadow bands” (partial folding of band dispersion) appear apparently as a result of short range AFM order. Formation of the so called Fermi “arcs” around Brillouin zone (BZ) diagonal reminiscent of the parts of noninteracting FS is experimentally detected in numerous ARPES

experiments². Despite apparently the same physics behind, pseudogap regime demonstrates some material specific features. For Bi2212 Fermi “arcs” go almost up to BZ border where they are strongly blurred. The NCCO also has Fermi “arcs” but FS “destruction” looks different. The “hot-spots” are well observed in NCCO while towards the BZ border FS is almost restored as a non interacting one.⁸

The present paper is devoted to pseudogap behavior in the underdoped LSCO and its comparison with Bi2212 and NCCO.

According to common knowledge high- T_c systems are usually doped Mott insulators, effectively described by the Hubbard model. Most common method to solve the Hubbard model in our days is dynamical mean-field theory (DMFT)⁹. Its exactness in the infinite spatial dimensions limit makes DMFT a local approach. Since high- T_c compounds as it is well established have quasi two-dimensional nature spatial fluctuations play important role for their physics. To overcome this difficulty we introduced DMFT+ $\Sigma_{\mathbf{k}}$ computational scheme^{10,11,12} which supplies conventional DMFT with “external” \mathbf{k} -dependent self-energy. Main assumption of the DMFT+ $\Sigma_{\mathbf{k}}$ is additive form of the self-energy which allows one to keep conventional DMFT self-consistent set of equations. The DMFT+ $\Sigma_{\mathbf{k}}$ approach was used to address the pseudogap problem¹¹, electron-phonon coupling in strongly correlated systems¹³ and disorder induced metal-insulator transition within the Hubbard-Anderson model¹⁴. For the pseudogap state this self-energy $\Sigma_{\mathbf{k}}$ describes the interaction of correlated electrons with non-local (quasi) static short-ranged collective Heisenberg-like antiferromagnetic (AFM or SDW-like) spin fluctuations¹⁵. DMFT+ $\Sigma_{\mathbf{k}}$ approximation was also shown to be appropriate to describe two-particle properties e.g. optical conductivity.¹⁶

As a possible way of theoretical simulation of the pseudogap regime for real materials we proposed LDA+DMFT+ $\Sigma_{\mathbf{k}}$ hybrid method⁷. It combines first principle one-electron density functional theory calculations within local density approximation (DFT/LDA)¹⁷ with DMFT+ $\Sigma_{\mathbf{k}}$.¹⁸

LDA+DMFT+ $\Sigma_{\mathbf{k}}$ method allowed us to obtain Fermi arcs and “hot-spots” behavior for both electron doped e.g. Nd_{1.85}Ce_{0.15}CuO₄⁸ (NCCO) and Pr_{1.85}Ce_{0.15}CuO₄ (PCCO)¹⁹ as well as hole doped Bi₂Sr₂CaCu₂O_{8- δ} (Bi2212)⁷ high-T_c cuprates. Pseudogap behavior of dynamic optical conductivity within LDA+DMFT+ $\Sigma_{\mathbf{k}}$ ¹⁶ was also discussed for Bi2212⁷ and NCCO⁸.

This communication reports LDA+DMFT+ $\Sigma_{\mathbf{k}}$ computations of Fermi surface and spectral functions for hole underdoped La_{1.86}Sr_{0.14}CuO₄ (LSCO) system supported by high energy, high resolution bulk sensitive ARPES³.

II. COMPUTATIONAL DETAILS

The La₂CuO₄ system has base-centered orthorhombic crystal structure with space group *Bmab* with two formula units per cell²⁰. Corresponding lattice parameters are $a=5.3346$, $a=5.4148$ and $c=13.1172$ Å. Atomic positions are the following: La(0.0,-0.0083,0.3616), Cu(0,0,0), O(1/4,1/4,-0.0084), O2(0.0,0.0404,0.1837).

As a first step of LDA+DMFT+ $\Sigma_{\mathbf{k}}$ method we performed density functional theory calculations in the local density approximation (LDA) for these crystallographic data. Band structure was obtained within the linearized muffin-tin orbitals (LMTO) method²¹. It is well known for these compounds that Fermi level is crossed by antibonding O2*p*-Cu3*d* partially filled orbital of $x^2 - y^2$ symmetry. Tight-binding parameters for this band were calculated by *N*-th order LMTO (NMTO) method²² as (in eV units) $t = -0.476$, $t' = 0.077$, $t'' = -0.025$, $t''' = -0.015$. These values agree well with previous studies.²³ Coulomb interaction value on effective Cu-3*d*($x^2 - y^2$) orbital was calculated by constrained LDA approach²⁴ and was found to be $U=1.1$ eV. These LDA obtained parameters are used to set up corresponding one-band Hubbard model.

The second step is further treatment of the above defined Hubbard model within the dynamical mean-field theory (DMFT) self-consistent set of equations⁹ supplied by “external” momentum-dependent self-energy $\Sigma_{\mathbf{k}}$ ¹¹. Using the additive form of self-energy (main approximation of the scheme neglecting the interference between Hubbard interaction and pseudogap fluctuations, which allows one to preserve conventional DMFT equations) one can define LDA+DMFT+ $\Sigma_{\mathbf{k}}$ Green function as:

$$G_{\mathbf{k}}(\omega) = \frac{1}{\omega + \mu - \varepsilon(\mathbf{k}) - \Sigma(\omega) - \Sigma_{\mathbf{k}}(\omega)} \quad (1)$$

where bare electron dispersion $\varepsilon(\mathbf{k})$ is defined by LDA calculated hopping parameters listed above. To calculate $\Sigma_{\mathbf{k}}$ we used a two-dimensional pseudogap model^{1,15}

describing nonlocal correlations induced by (quasi) static short-range collective Heisenberg-like AFM spin fluctuations. Thus we introduce correlation length dependence of the pseudogap fluctuations into conventional DMFT loop.

There are two points which make DMFT+ $\Sigma_{\mathbf{k}}$ different from the usual DMFT. First, momentum dependent $\Sigma_{\mathbf{k}}$ is recalculated on each DMFT iteration ($\Sigma_{\mathbf{k}}(\mu, \omega, [\Sigma(\omega)])$) is in fact the function of DMFT chemical potential and DMFT self-energy). Second, DMFT+ $\Sigma_{\mathbf{k}}$ lattice problem is defined at each DMFT iteration as:

$$G_{ii}(\omega) = \frac{1}{N} \sum_{\mathbf{k}} \frac{1}{\omega + \mu - \varepsilon(\mathbf{k}) - \Sigma(\omega) - \Sigma_{\mathbf{k}}(\omega)}. \quad (2)$$

After numerical self-consistency is reached we get the Green’s function (1) with corresponding $\Sigma(\omega)$ and $\Sigma_{\mathbf{k}}(\omega)$ taken on the last DMFT iteration. All further computational details can be found e.g. in Refs. 7,8,11.

As an “impurity solver” for DMFT equations numerical renormalization group (NRG^{25,26}) was employed. Temperature of DMFT(NRG) computations was taken to be 0.011 eV and electron concentration used was $n=0.86$.

Self-energy $\Sigma_{\mathbf{k}}(\omega)$ due to pseudogap fluctuations depends, in general, on two parameters: the pseudogap amplitude Δ , and the correlation length ξ .^{1,15} The value of Δ was calculated as in Ref. 11

$$\Delta^2 = U^2 \frac{\langle n_{i\uparrow} n_{i\downarrow} \rangle}{n^2} < (n_{i\uparrow} - n_{i\downarrow})^2 \rangle, \quad (3)$$

where local densities $n_{i\uparrow}$, $n_{i\downarrow}$ and double occupancy $\langle n_{i\uparrow} n_{i\downarrow} \rangle$ were calculated within the standard DMFT⁹. Behavior of Δ as a function of hopping integrals and Coulomb interaction was studied in our previous work¹¹, while Δ as a function of occupancy n was investigated in Ref. 7. For ξ we believe it is more safe to take experimental values. In this work the value of Δ was calculated to be 0.275 eV and ξ was taken to be $10a$, where a - lattice constant.²⁷

III. EXPERIMENTAL DETAILS

The high-energy ARPES measurements were carried out at BL25SU in SPring- 8, using incident photons of 500 eV, on single crystal samples. The normal to the cleaved sample surface was set almost parallel to the axis of the lens of the analyzer and the sample was set to about 45° from the incident light direction. The photoelectrons within polar angles of about $\pm 6^\circ$ around the normal to the sample were simultaneously collected using a GAMMADATASCIENTA SES200 analyzer, thereby covering more than a whole Brillouin zone along the directions of the analyzer slit. The Fermi surface mapping was performed by changing the angle along the perpendicular direction to the analyzer slit. The base pressure was about 4×10^{-8} Pa. The (001) clean surface was obtained by cleaving the samples in situ in vacuum

at the measuring temperature of 20 K. The overall energy resolution was set to 100 and 170 meV for high-resolution measurements and Fermi surface mapping, respectively. The angular resolution was ± 0.1 (± 0.15) for the perpendicular (parallel) direction to the analyzer slit. These values correspond to the momentum resolution of $\pm 0.024\pi/a$ ($\pm 0.036\pi/a$) at $h\nu=500$ eV, where a is twice the Cu-O bondlength within the CuO_2 plane. By virtue of the longer photoelectron mean free path of ~ 12 Å at the kinetic energy of ~ 500 eV than that for conventional ARPES at $h\nu \sim 20$ -60 eV, the bulk contribution to the spectral weight is estimated as about 60%. The position of the Fermi level was calibrated with Pd spectra.

IV. RESULTS AND DISCUSSION

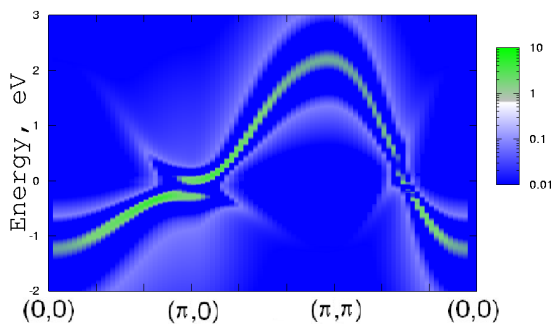


FIG. 1: LCOO $\text{Cu-}3d(x^2 - y^2)$ band dispersion along high symmetry directions of square Brillouin zone computed with LDA+DMFT+ $\Sigma_{\mathbf{k}}$. The Fermi level is zero.

In case of finite temperature and interaction strength we have to take into account the finite life time effects of quasiparticles. Thus instead of just a dispersions $\varepsilon(\mathbf{k})$ one should rather work with the spectral function $A(\omega, \mathbf{k})$ given by

$$A(\omega, \mathbf{k}) = -\frac{1}{\pi} \text{Im}G(\omega, \mathbf{k}), \quad (4)$$

with retarded Green's function $G(\omega, \mathbf{k})$ obtained via LDA+DMFT+ $\Sigma_{\mathbf{k}}$ scheme^{10,11,16}. Of course there are considerable lifetime effects originating from the $\Sigma_{\mathbf{k}}$ corresponding to interaction with AFM fluctuations (substituted in our approach by the quenched random field).

In Fig. 1 contour map of spectral function (4) obtained from LDA+DMFT+ $\Sigma_{\mathbf{k}}$ for $\text{Cu-}3d(x^2 - y^2)$ band is presented. The width of the spectral function is inversely proportional to the lifetime. Around $(\pi, 0)$ point one can clearly see splitting of the spectra by AFM pseudogap fluctuations of the order of 2Δ . Also AFM nature of the pseudogap fluctuations leads to formation of the “shadow” band which is much weaker in intensity and becoming the real quasiparticle band in case of complete folding in case of long-range AFM order.

Figure 2 displays experimental energy distribution curves (EDC) on the panel (a) along $(0,0)$ - $(\pi,0)$ direc-

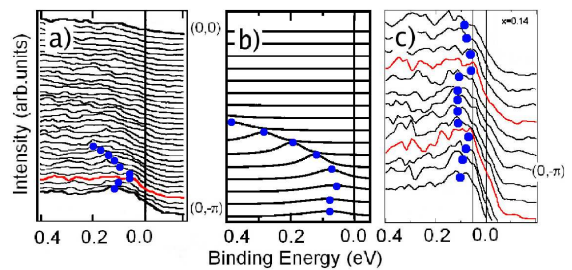


FIG. 2: ARPES EDC curves (a) and LDA+DMFT+ $\Sigma_{\mathbf{k}}$ spectral functions (b) along $(0,0)$ - $(\pi, 0)$ high symmetry direction; (c) ARPES MDC curves around $(\pi, 0)$ point for LSCO at $x=0.14$. On panels (a), (b) and (c) filled circles guide the motion of the $A(\omega, \mathbf{k})$ maxima. The Fermi level is zero.

tion. Around $(\pi, 0)$ -point as shown by stars certain deviation of the $A(\omega, \mathbf{k})$ maxima from the Fermi level a kind of “turn-back” is observed. We attribute such behavior of the $A(\omega, \mathbf{k})$ to pseudogap fluctuations. Similar theoretical behavior is shown on panel (b)²⁸ of Fig. 2 as calculated by our LDA+DMFT+ $\Sigma_{\mathbf{k}}$ approach (see also Fig. 1). The same behavior is also observed as traced by circles in experimental ARPES momentum distribution curves (MDC) demonstrated on panel (c) of Fig. 2.

The bulk-sensitive high-energy ARPES data for $\text{La}_{1.86}\text{Sr}_{0.14}\text{CuO}_4$ show a clear “turn-back” structure of the EDC peak as a function of momentum near $(0, -\pi)$, which were not seen in the previous low-energy ARPES data for $\text{La}_{1.85}\text{Sr}_{0.15}\text{CuO}_4$ ⁴. The contour map of the spectral weight in the vicinity of E_F seems to be essentially similar in overall features for this doping level between the high-energy and low-energy ARPES studies.

Experimental and theoretical Fermi surface maps are shown in Fig. 3 at panels (a) and (b) correspondingly. Both pictures reveal strong scattering around $(\pi, 0)$ -point which we associate with scattering in the vicinity of the so-called “hot-spots” (cross-points of a Fermi and AFM umklapp surfaces) which are close to the $(\pi, 0)$ ^{7,8}. Such strong scattering comes from scattering processes with momentum transfer of the order of $\mathbf{Q}=(\pi, \pi)$ ^{1,15}, corre-

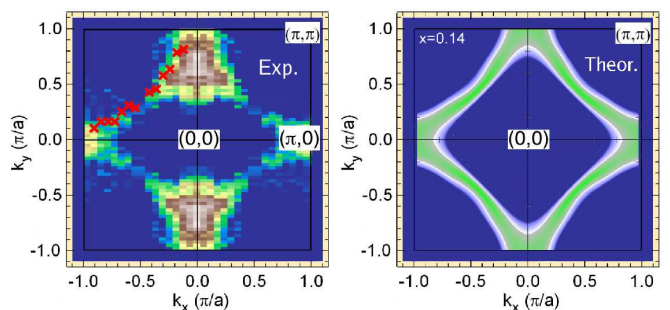


FIG. 3: Fermi surfaces of LSCO at $x=0.14$ from experiment (left panel) and LDA+DMFT+ $\Sigma_{\mathbf{k}}$ computations (right panel) Red crosses on the left panel correspond to experimental \mathbf{k}_F values.

sponding to AFM pseudogap fluctuations. Along nodal directions we observe typical Fermi arcs. They are pretty well seen in the theoretical data while for experiment we have just narrow traces of them.

V. CONCLUSION

Our LDA+DMFT+ $\Sigma_{\mathbf{k}}$ hybrid approach was shown to be an effective numerical tool to describe short-range ordered state in quasi-two dimensional systems.^{7,8,19} Material specific model parameters such as hopping integrals (which define bare electronic band dispersion of effective $\text{Cu}3d(x^2 - y^2)$ orbital) were calculated via LDA based NMTO method.²² Coulomb interaction parameter U was obtained from constrained LDA method. Pseudogap amplitude Δ was computed using LDA+DMFT scheme.^{8,11} Supplementing conventional DMFT self-energy by $\Sigma_{\mathbf{k}}(\omega)$ describes non-local dynamical correlations due to short ranged collective Heisenberg like AFM spin fluctuations.

In this work we performed LDA+DMFT+ $\Sigma_{\mathbf{k}}$ calculations for hole-doped $\text{La}_{1.84}\text{Sr}_{0.14}\text{CuO}_4$ compound in the pseudogap regime. Because of fluctuations of AFM short-range order we clearly observe formation of the so called “shadow bands” as partially folded bare dispersion. Pseudogap is formed around $(\pi, 0)$ point which is qualitatively the same as in $\text{Bi}2212^7$, NCCO^8 and PCCO^{19} . As to Fermi surface of LSCO it is alike that obtained for $\text{Bi}2212^7$. Namely the “hot spots” are not well resolved

since the crossing point of the bare Fermi surface and AFM umklapp surface are very close to Brillouin zone border. This fact is essentially due to the shape and size of LDA Fermi surface. In this respect, situation here is different from that for NCCO^8 and PCCO^{19} , where “hot spots” are clearly seen. To support these theoretical results we present here the new high energy, high resolution ARPES data for LSCO. Typical pseudogap-like effects of Fermi surface destruction were observed in both theory and experiment. The same is true for spectral functions. The overall semiquantitative agreement between theory and experiments basically supports our general picture of the pseudogap state as due to strong scattering of carriers by short-range AFM order fluctuations.

VI. ACKNOWLEDGEMENTS

We thank Thomas Pruschke for providing us the NRG code. This work is supported by RFBR grants 08-02-00021, 08-02-91200, RAS programs “Quantum physics of condensed matter” and “Strongly correlated electrons solids”. IN is supported by Grants of President of MK-614.2009.2(IN) and Russian Science Support Foundation. AS and SS acknowledge JSPS for the financial support for the Japan-Russia collaborating research in 2008-09. They also acknowledge MEXT, Japan for the support in Grant-in-Aid for scientific Research (18104007, 15GS0123, 18684015).

-
- ¹ T. Timusk, B. Statt, Rep. Progr. Phys., **62**, 61 (1999); M. V. Sadvovskii, Usp. Fiz. Nauk **171** 539 (2001) [Phys. Usp. **44**, 515 (2001)]; M. V. Sadvovskii, in “Strings, branes, lattices, networks, pseudogaps and dust”, Scientific World, Moscow, 2007, p. 357 (in Russian), English version: cond-mat/0408489.
- ² A. Damascelli, Z. Hussain, and Zhi-Xun Shen, Rev. Mod. Phys. **75**, 473 (2003).
- ³ M. Tsunekawa, A. Sekiyama, S. Kasai, S. Imada, H. Fujiwara, T. Muro, Y. Onose, Y. Tokura and S. Suga, New J. Phys. **10**, 073005 (2008).
- ⁴ T. Yoshida, X. J. Zhou, K. Tanaka, W. L. Yang, Z. Hussain, Z.-X. Shen, A. Fujimori, S. Sahrakorpi, M. Lindroos, R. S. Markiewicz, A. Bansil, Seiki Komiya, Yoichi Ando, H. Eisaki, T. Kakeshita, and S. Uchida, Phys. Rev. B **74**, 224510 (2006).
- ⁵ V. J. Emery, S. A. Kivelson, Nature **374**, 434 (2002).
- ⁶ A. A. Kordyuk, S. V. Borisenko, V. B. Zabolotnyy, R. Schuster, D. S. Inosov, D. V. Evtushinsky, A. I. Plyushchay, R. Follath, A. Varykhalov, L. Patthey, and H. Berger, Phys. Rev. B **79**, 020504(R) (2009).
- ⁷ E. Z. Kuchinskii, I. A. Nekrasov, Z. I. Pchelkina, M. V. Sadvovskii, Zh. Eksp. Teor. Fiz. **131**, 908 (2007) [JETP **104**, 792 (2007)]; I. A. Nekrasov, E. Z. Kuchinskii, Z. V. Pchelkina and M. V. Sadvovskii, Physica C **460-462**, 997 (2007).
- ⁸ E. E. Kokorina, E. Z. Kuchinskii, I. A. Nekrasov, Z. V. Pchelkina, M. V. Sadvovskii, A. Sekiyama, S. Suga, M. Tsunekawa. Zh. Eksp. Teor. Fiz. **134**, 968 (2008) [JETP **107**, 818 (2008)]; I. A. Nekrasov *et al.*, J. Phys. Chem. Solids **69**, 3269 (2008).
- ⁹ A. Georges, G. Kotliar, W. Krauth and M. J. Rozenberg, Rev. Mod. Phys. **68**, 13 (1996).
- ¹⁰ E. Z. Kuchinskii, I. A. Nekrasov, M. V. Sadvovskii, Pis'ma ZhETF **82**, 217 (2005) [JETP Lett. **82**, 198 (2005)].
- ¹¹ M. V. Sadvovskii, I. A. Nekrasov, E. Z. Kuchinskii, Th. Pruschke, V. I. Anisimov. Phys. Rev. B **72**, 155105 (2005).
- ¹² E. Z. Kuchinskii, I. A. Nekrasov, M. V. Sadvovskii, Fizika Nizkikh Temperatur **32** (2006) 528 [Low Temperature Physics **32** (2006) 398].
- ¹³ E. Z. Kuchinskii, I. A. Nekrasov, M. V. Sadvovskii, Phys. Rev. B **80**, 115124 (2009).
- ¹⁴ E. Z. Kuchinskii, I. A. Nekrasov, M. V. Sadvovskii, Zh. Eksp. Teor. Fiz. **133**, 670 (2008) [JETP **106**, 581 (2008)].
- ¹⁵ J. Schmalian, D. Pines, B. Stojkovic, Phys. Rev. B **60**, 667 (1999); E. Z. Kuchinskii, M. V. Sadvovskii, Zh. Eksp. Teor. Fiz. **115**, 1765 (1999) [JETP **88**, 347 (1999)].
- ¹⁶ E. Z. Kuchinskii, I. A. Nekrasov, M. V. Sadvovskii, Phys. Rev. B **75** 115102 (2007).
- ¹⁷ R. O. Jones and O. Gunnarsson, Rev. Mod. Phys. **61**, 689 (1989).
- ¹⁸ K. Held, I. A. Nekrasov, G. Keller, V. Eyert, N. Blumer, A. K. McMahan, R. T. Scalettar, Th. Pruschke, V. I. Anisimov, and D. Vollhardt, Psi-k Newsletter **56**, 65 (2003) [psi-k.dl.ac.uk/newsletters/News_56/Highlight_56.pdf]; K. Held, Adv. Phys. **56**, 829 (2007)

- ¹⁹ I.A. Nekrasov, N.S. Pavlov, E.Z. Kuchinskii, M.V. Sadovskii, Z.V. Pchelkina, V.B. Zabolotnyy, J. Geck, B. Buchner, S.V. Borisenko, D.S. Inosov, A.A. Kordyuk, M. Lambacher, A. Erb, Phys. Rev. B **80** 115124(R) (2009).
- ²⁰ M. Braden, P. Schweiss, G. Heger, W. Reichardt, Z. Fisk, K. Gamayunov, I. Tanaka, H. Kojima, Physica C **223**, 396 (1994).
- ²¹ O. K. Andersen, Phys. Rev. B **12**, 3060 (1975); O. K. Andersen and O. Jepsen, Phys. Rev. Lett. **53**, 2571 (1984).
- ²² O. K. Andersen and T. Saha-Dasgupta, Phys. Rev. B **62**, R16219 (2000); O. K. Andersen *et al.* Psi-k Newsletter **45**, 86 (2001); O. K. Andersen, T. Saha-Dasgupta, S. Ezhov, Bull. Mater. Sci. **26**, 19 (2003).
- ²³ Korshunov M.M., Gavrichkov V.A., Ovchinnikov S.G., Pchelkina Z.V., Nekrasov I.A., Korotin M.A., Anisimov V.I., Zh. Eksp. Teor. Fiz. **126**, 642 (2004) [JETP **99**, 559 (2004)].
- ²⁴ O. Gunnarsson, O. K. Andersen, O. Jepsen, and J. Zaanen, Phys. Rev. B **39**, 1708 (1989).
- ²⁵ K. G. Wilson, Rev. Mod. Phys. **47**, 773 (1975); H. R. Krishna-murthy, J. W. Wilkins, and K. G. Wilson, Phys. Rev. B **21**, 1003 (1980); *ibid.* **21**, 1044 (1980).
- ²⁶ R. Bulla, A. C. Hewson and Th. Pruschke, J. Phys.: Condens. Matter **10**, 8365 (1998);
- ²⁷ M. Hcker, Young-June Kim, G. D. Gu, J. M. Tranquada, B. D. Gaulin, J. W. Lynn, Phys. Rev. B **71**, 094510 (2005).
- ²⁸ Theoretical curves are shifted up by 0.2 eV for better agreement with experiment.